COMPTEL Solar Flare Observations

J.M. Ryan[3], H. Aarts[2], K. Bennett[4], H. Debrunner[5], C. de Vries[2], J.W. den Herder[2], G. Eymann[4], D.J. Forrest[3], R. Diehl[1], W. Hermsen[2], R. Kippen[3], L. Kuiper[2], J. Lockwood[3], M. Loomis[3], G. Lichti[1], J. Macri[3], M. McConnell[3], D. Morris[3], V. Schönfelder[1], G. Simpson[3], M. Snelling[4], H. Steinle[1], A. Strong[1], B.N. Swanenburg[2], W.R. Webber[3], and C. Winkler[4]

[1]Max-Planck Institut für Extraterrestrische Physik, Garching, Germany

[2]Laboratory for Space Research Leiden, PB 9504, 2300 RA Leiden, The Netherlands

[3]Space Science Center,Institute for the Study of Earth, Oceans and Space University of New Hampshire Durham, NH

[4]Space Science Division of ESA, ESTEC, Noordwijk, The Netherlands

[5]University of Bern, Bern, Switzerland

COMPTEL as part of a solar Target of Opportunity campaign observed the sun during the period of high solar activity from 7 June to 15 June 1991. Major flares were observed on June 9 and 11. Although, both flares were large GOES events (≥ X10), they were not extraordinary in terms of γ-ray emission. Only the decay phase of the June 15 flare was observed by COMPTEL. We report the preliminary analysis of data from these flares, including the first spectroscopic measurement of solar flare neutrons. The deuterium formation line at 2.223 MeV was present in both events, and for at least the June 9 event, was comparable to the flux in the nuclear line region of 4 - 8 MeV, consistent with SMM observations. A clear neutron signal was present in the flare of 9 June with the spectrum extending up to 80 MeV and consistent in time with the emission of γ-rays, confirming the utility of COMPTEL in measuring the solar neutron flux at low energies. The neutron flux below 100 MeV appears to be lower than that of the 1982 June 3 flare by more than an order of magnitude. The neutron signal of the 11 June event is under study. Severe dead time effects resulting from the intense thermal X-rays require significant corrections to the measured flux which increase the magnitude of the associated systematic uncertainties.

1. Introduction

As a secondary scientific objective of the COMPTEL γ-ray telescope on the Arthur Holly Compton Gamma Ray Observatory, observing and measuring solar flares assumed an unexpected importance due to the unusually high level of solar activity early in the mission. During the two week period of 1991 June 1 to June 15 region 6659 (Boulder reference number) transited the disk producing an unprecedented number of large flares. After the first week of this activity, the prospect of more flares was such that the sun was declared a Target of Opportunity and on June 7 the observation of the Cygnus region was suspended and the Compton Observatory was reoriented so as to place the sun near the spacecraft *z* axis. Since the spacecraft *z* axis coincides with the axis of the COMPTEL field-of-view, this enabled COMPTEL to utilize its full capabilities in measuring the gamma ray and neutron fluxes from the flares which occurred the following week. Major flares were recorded on June 9, 11 and 15 after which the Compton Observatory re-assumed its original objective of the all-sky survey.

2. COMPTEL γ-Ray and Neutron Response

COMPTEL is a two element γ-ray detector in which the Compton scattering process is used to measure the photon's energy and incident direction. Similarly, it can also detect and measure neutrons. However, rather than using Compton scattering, neutron detection relies upon neutron-proton scattering. Both forms of neutral radiation are important in studying high energy solar flare processes. A description of the instrument and its in-flight performance is given by den Herder *et al.* (1991).

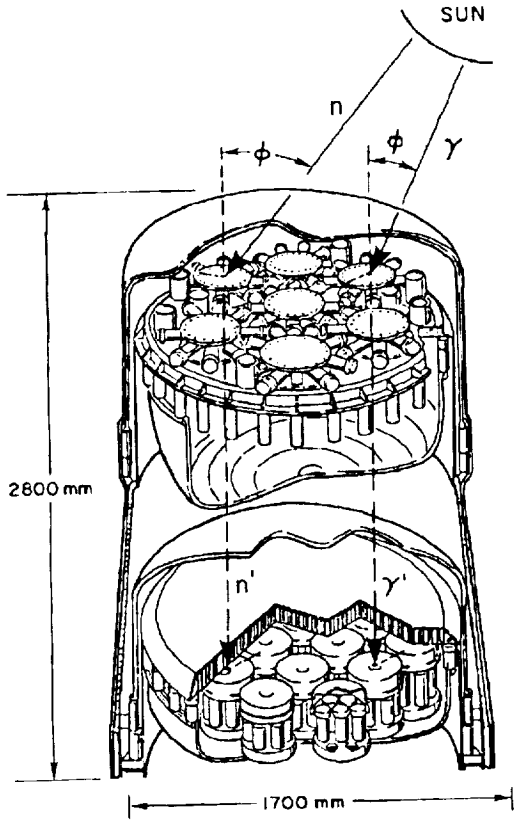

Figure 1. Schematic of COMPTEL showing the interactions of γ-rays and neutrons. The scatter angle ϕ for γ-rays is given by $\phi = \cos^{-1}(1 - \varepsilon/E_2 + \varepsilon/(E_1 + E_2))$; where ε = 511 keV. The non-relativistic hard sphere, neutron-proton scattering formula is $\tan^2 \phi = E_1/E_s$.

The basic scattering process for photons (and neutrons) is illustrated in Fig. 1. The quantities that COMPTEL measures are the location of the scatter in the seven element forward detector D1, the energy E_1 of the scattered electron (proton), the location of the scatter in the fourteen element rearward detector D2 and the energy deposit E_2 in that detector. One computes

from these interaction locations the direction of the scattered photon's (neutron's) velocity vector. For γ-rays, one computes the scatter angle ϕ and the total γ-ray energy ($E_1 + E_2$), where

$$\phi = \cos^{-1}(1 - \varepsilon/E_2 + \varepsilon/(E_1 + E_2)).$$

Here, ε is the electron rest mass energy and ϕ is the Compton scatter angle provided $E_1 + E_2$ is the full incident γ-ray energy. Without measuring the direction of the scattered electron in D1, only the polar angle and not the azimuth angle of the scatter is known. The time-of-flight (TOF) is also measured and used to help identify γ-ray scatters; whereas for neutron detection, it is used to measure the energy of the scattered neutron.

Much like a γ-ray event, the ideal type of neutron interaction in COMPTEL occurs when the incoming neutron elastically scatters off a hydrogen nucleus in the D1 detector. The scattered neutron then proceeds to the D2 detector where it interacts, depositing some of its energy to produce a trigger signal as indicated in Figure 1. The energy of the incident neutron is computed by summing the proton recoil energy E_1 in the D1 detector with the energy of the scattered neutron E_s deduced from the TOF from the D1 to the D2 detector. The scatter angle for non-relativistic neutrons (< 100 MeV) can be computed by the formula:

$$tan^2 \phi = E_1/E_s .$$

Relativistic corrections become important above 100 MeV, in which case the expression becomes

$$tan^2\phi = \frac{E_1/E_s}{1 + E_n/2m_n},$$

where $E_n = E_1 + E_s$ is the incident neutron kinetic energy.

The material in D1 is a liquid organic scintillator, NE213A, with the properties of low density and low Z (H/C ratio = 1.286). The material elastically scatters both γ-rays and neutrons off atomic electrons and hydrogen nuclei, respectively. The detector thickness has been chosen such that it is a fraction of a mean free path thick, meaning that the incident γ-ray (or neutron) can scatter in D1 and usually leave D1 without scattering again.

The liquid organic scintillator in D1 (NE213A) possesses pulse shape discrimination properties, in that energetic protons produce light pulses with longer rise times than those of electrons (and other minimum ionizing particles). This capability allows for efficient identification of recoil proton signals produced by fast neutrons elastically scattering off hydrogen in D1. Any reaction producing a recoil proton can be identified by these means, such as inelastic scattering of fast neutrons off carbon producing a γ-ray and either a knock-on proton or neutron (which can then elastically scatter off hydrogen). Pure γ-ray producing neutron-carbon reactions in D1 also occur and represent an intrinsic background in both γ-ray and neutron measurements.

Since only the scatter angle ϕ is measured, the incident particle direction is constrained to a cone mantle of half angle ϕ. For γ-rays, errors in the measured energy and placement of the cone mantle occur via uncertainties in the measured energies in D1 and D2 and uncertainties in the measured interaction positions. Partial energy absorption in D2 (from an escaping γ-ray) yields a low value for the total γ-ray energy and a large value for the scatter angle ϕ. Similar errors are inherent in the neutron measurement as well, except that the TOF resolution is the primary component in the scattered neutron energy uncertainty. The neutron energy resolution (σ) of about 6% results in an uncertainty in the production time of the neutron at the sun of ~ 1 minute for a 40 MeV neutron.

Since a full γ-ray energy deposit in D2 is necessary to obtain a correct measure of the scatter angle ϕ, we have a means for selecting only photopeak events in the data. For a solar flare γ-ray interacting in COMPTEL, the inferred scatter angle ϕ about the vector of the scattered γ-ray should be such that the photon is assigned a solar origin as indicated schematically in Figure 1. Hence, we know that the photon deposited its full energy in the detector. The response of the telescope to such events is simple. The energy or pulse height distribution is basically Gaussian in shape with a heavily suppressed Compton tail at low energies. Since the solar γ-ray spectra are rich in lines from C, N, O, Ne, Mg etc., a simple instrumental response function will facilitate correct de-convolution of the pulse height spectra. The response of a telescope prototype to monoenergetic 1.375 and 2.75 MeV photons from a ^{24}Na source is shown in Figure 2.

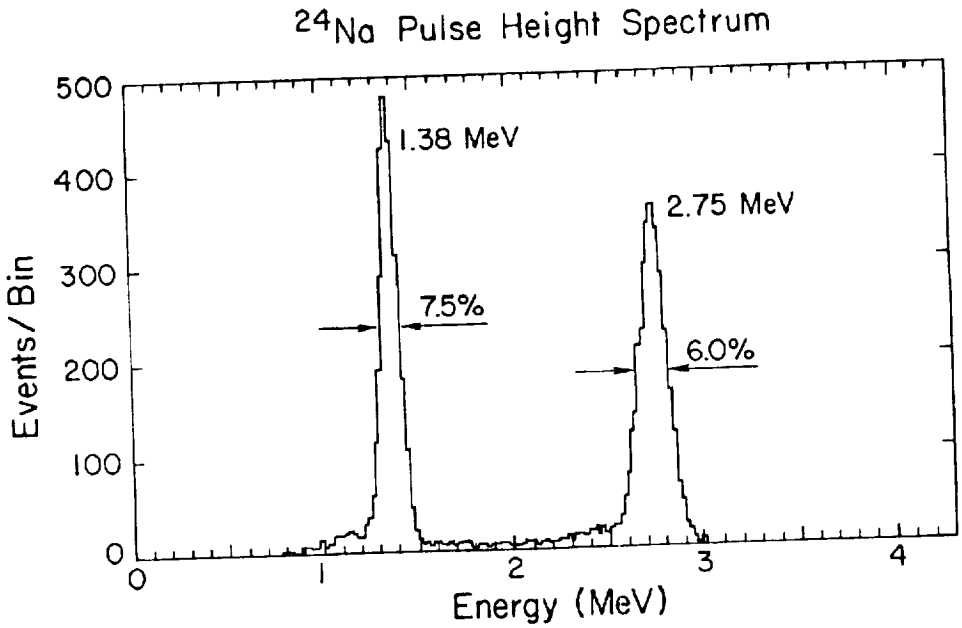

Figure 2.
The energy spectrum from a monoenergetic γ-ray source produced under the constraint that the γ-ray scatter angle ϕ be consistent with the source direction.

Similarly, in detecting and measuring neutrons from the sun the neutrons can be traced backwards from D2 to D1 through the angle ϕ onto a cone mantle restricting the incident direction so as to include the sun. This geometrical constraint is identical to that of the γ-ray measurements. For neutrons, energy is more often lost in D1 through inelastic scatters with carbon with consequent indeterminate scattering kinematics. Such reactions are suppressed by requiring a scatter angle ϕ which is consistent with the solar direction.

4. γ-ray Flare Overview

γ-ray emission was detected from at least three flares observed by COMPTEL in the June 1991 solar Target of Opportunity observation. Shown in Figure 3 is the time-intensity profile above 1 MeV and the count spectrum of the June 9 solar flare. This event, as well as the flare on June 11, lasted on the order of 10 minutes above 1 MeV and both show evidence of nuclear line emission, particularly at the deuterium formation line of 2.223 MeV. Images of the sun were produced with these data and were of sufficient angular resolution to show the

apparent motion of the sun over the course of two days. Figure 4 is the COMPTEL image of the sun on June 9 during the impulsive phase of the flare. The angular resolution of COMPTEL is on the order of one degree while the diameter of the sun is one half that, so the images do not reveal any information on the location of the γ-ray emission on the solar disk. The flare on June 15 was not observable until about 0900 UT, approximately 40 minutes after the X-ray maximum. Before this the spacecraft was in orbit night or in the South Atlantic Anomaly. However, an image of the sun could still be constructed, supporting the conclusion of Akimov *et al.* (1991) of prolonged (> 1 hour) γ-ray emission from this flare.

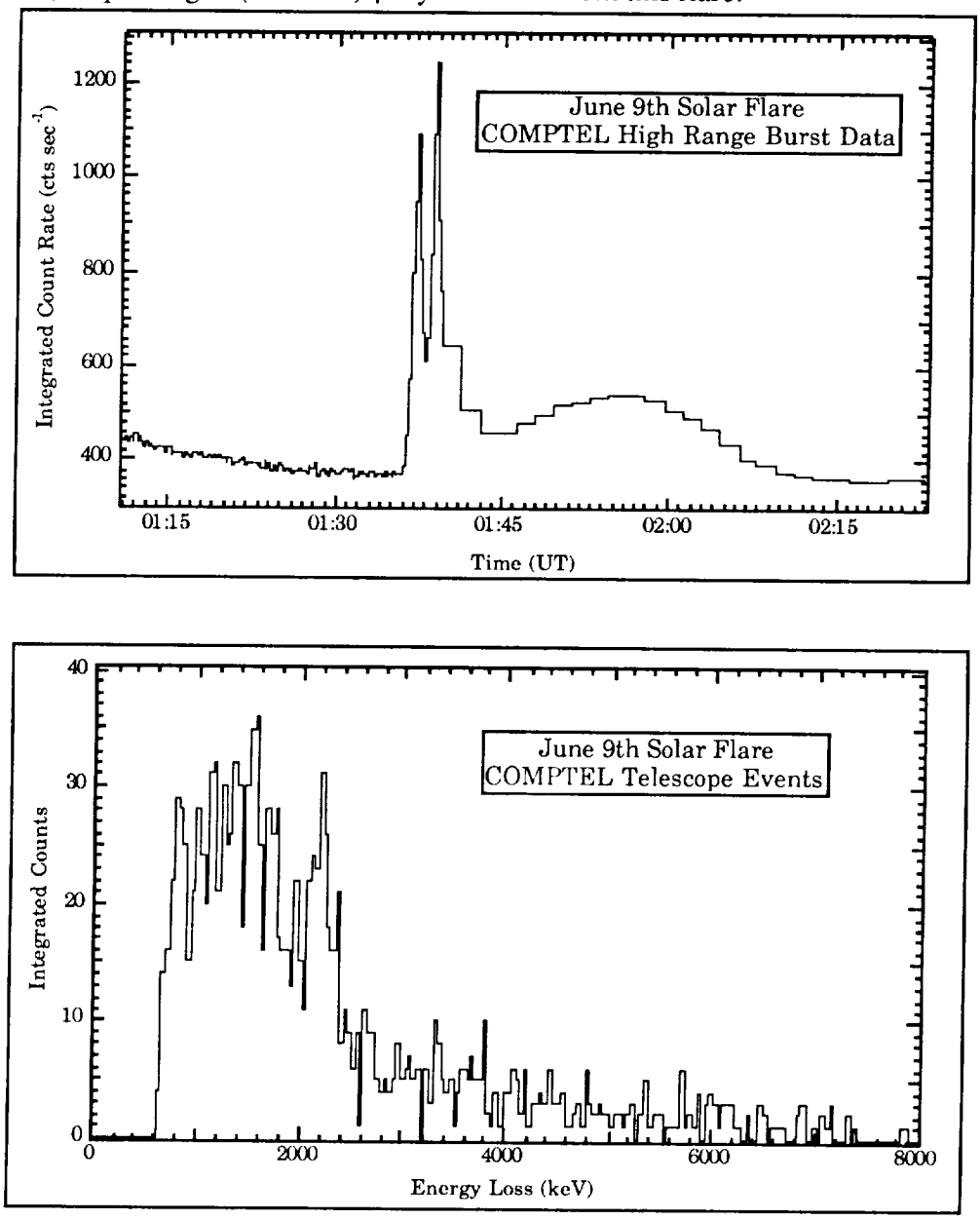

Figure 3. The intensity-time profile > 1 MeV and the time-integrated count spectrum from the solar flare of 1991 June 9.

The intense solar flare on June 4 was also measured by COMPTEL, although the sun was not in the field-of-view. The COMPTEL burst detector system measured the γ-ray spectrum above 1 MeV. The burst detector was occulted by other components of the spacecraft, so that the de-convolution of the count rate spectrum will be more complex than for the flares in the field-of-view. This flare emitted a flux of neutrons which was detectable at ground level at Mt. Norikura in Japan (Muraki *et al.* 1991).

5. Analysis of the 1991 June 9 Solar Flare

Only the June 9 flare which occurred during the Target of Opportunity period has been analyzed in any detail. The analysis includes both γ-rays and neutrons.

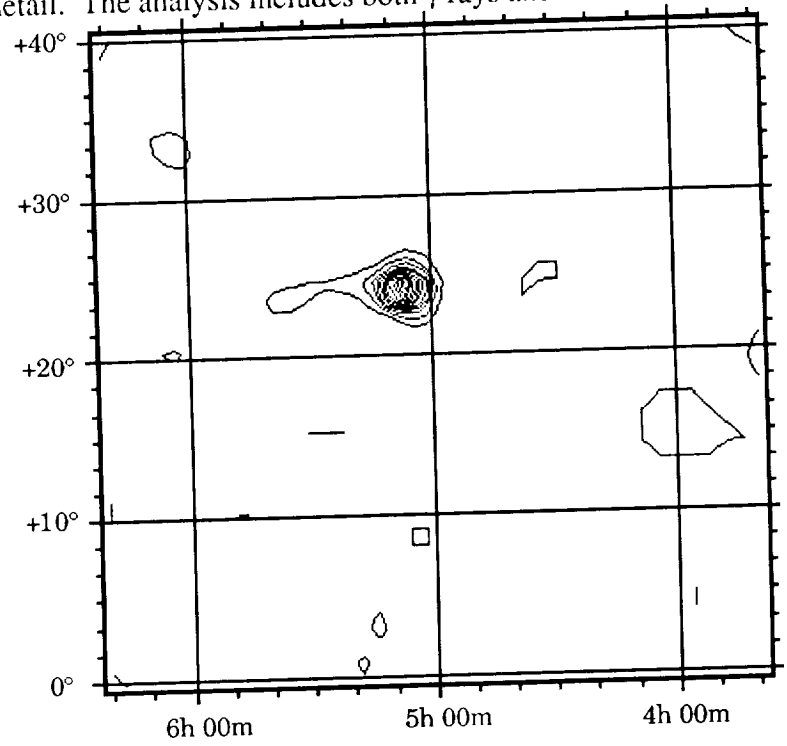

Figure 4. The COMPTEL image of the sun taken during the impulsive phase of the flare. The coordinates are declination as Right Ascension. The image is consistent with a point source response. The correct solar position is α = 5h 07m and δ = 22.9°.

5a. γ-Ray Analysis

The June 9 flare (3B, X10.0) occurred in active region 6659 at N34E04 with the X-ray start at 0134 UT and maximum at 0143 UT. From the COMPTEL data we define the impulsive phase to be from 0136 UT to 0146 UT. The γ-ray intensity-time profile is shown in Figure 3. These data were obtained from the COMPTEL high range burst detector which has a threshold of ~ 1 MeV. The broad maximum near 0158 UT is due only to the increased background count rate from the spacecraft excursion to higher latitudes in the course of its orbit. The telemetry of COMPTEL is basically divided into two separate channels, denoted γ1 and γ2 with γ1 being devoted to γ-rays of the highest quality (most amenable to analysis). The γ2 channel which is normally used for background studies is tailored to accept solar neutrons during flares. During

the impulsive phase the γ-ray count rate was high, filling up the γ1 telemetry channel and precluding the transmission of any γ2 events. During this same time interval the activity in the forward veto detector V1 was high as well. This was due to the intense thermal X-ray flux at a few keV piling up in V1, continuously triggering that detector and producing a large and variable dead time effect in COMPTEL. The thermal X-ray flux remained high, well beyond the impulsive phase. This required additional analysis to estimate the dead time for both the impulsive phase and the period of time afterward during which we expect the arrival of solar neutrons. The dead time correction was estimated by the throughput of LED calibration events in D1 during the impulsive phase and the period afterward. During the impulsive phase the average live time fraction was (28 ± 1)%, while from 0146 to 0205 UT the effect was (78 ± 4)%.

In the analysis of the γ-ray data it is important to estimate both the integrated flux of the 2.223 MeV emission from deuterium formation and the integrated flux in the nuclear line region of 4 - 8 MeV. The emission of the 2.2 MeV line depends upon the number of free, low energy neutrons within the photosphere, while emission in the broad nuclear line region depends upon the energy spectrum of protons above 30 MeV as they interact with the solar atmosphere. Since the production cross sections of neutrons and nuclear lines have very different energy dependences, the comparison of the γ-ray emission at 2.2 MeV and in the range of 4 - 8 MeV is a useful indicator of the parent proton spectral shape (Murphy and Ramaty 1984).

The broad band efficiency from 4 - 8 MeV was estimated by a Monte Carlo simulation calculation under the same restrictions as imposed on the real data. The instrument efficiency in the line at 2.2 MeV was obtained through interpolation of calibration simulations, again with restrictions similar to those applied to the real data. Using both the live time estimates and the estimates of the telescope efficiencies, we calculate from the time-integrated count rate spectrum (Fig. 3) the time-integrated fluxes to be 32 and 35 $\gamma\text{-cm}^{-2}$ for the the γ-ray emission in the range of 4 - 8 MeV and in the 2.223 MeV line, respectively. The uncertainties for these quantities are estimated to be 50 and 30%, respectively. The uncertainties are largely determined by the systematic errors in the estimated efficiencies rather than by dead time corrections or statistics. No other spectral analysis has been performed, although there is evidence for other identifiable lines in the spectrum.

5b. Neutron Analysis

Additional processing must take place in the neutron data analysis. All the quantities normally measured and telemetered are in terms of γ-ray interactions. Quantities appropriate to neutrons must be computed. These include (1) converting the electron-equivalent energy measured in D1, the upper liquid organic scintillator, into the proton-equivalent energy, (2) calculating the energy of the scattered neutron (from D1 to D2) from the time-of-flight, (3) computing the scatter angle ϕ from the n-p scattering kinematics, (4) discarding events which have electron-recoil pulse shape signatures in D1 and (5) discarding events which fall within the γ-ray time-of-flight window. The neutron differential flux can then be calculated based upon the data satisfying these criteria along with the live time and the neutron detection efficiency.

Presently, the best figures for the COMPTEL neutron detection efficiency are the extrapolations of the COMPTEL prototype neutron measurements to the full COMPTEL configuration. The calibrations were performed at only a few energies and incident angles (Ryan *et al.* 1987). The efficiencies needed for the flux calculations were interpolated between calibration points. The differential flux was calculated taking into account the limited number of operating detectors and the live time during the neutron measurements.

In principle the data restrictions listed above coupled with data restrictions that are usually used for γ-ray spectral studies should be all that is required to derive a solar neutron spectrum and intensity-time profile. The main selection criterion needed for spectral studies is that the scatter angle ϕ of an event be consistent with the position of the sun. This means that

the event circle whose center is defined by the velocity vector of the scattered neutron and whose diameter is defined by the scatter angle, comes within, in this case, 10° of the sun. This requirement implies that the measured energy is correct since in Compton telescopes the imaging and spectral analysis properties are intertwined. The amount of background which needs to be identified and adjusted for was unknown prior to the launch of the GRO.

We found that the usual data restrictions were inadequate to reject all background neutrons. One can propagate the potential solar neutrons backward, taking out neutron velocity dispersion effects, to calculate the production time at the sun in order to compare with the same quantity for γ-rays. By doing this, we found that many neutron events originated before the solar γ-rays and that neutron production extended beyond the end of the impulsive phase (once the time-of-flight of the γ-rays over 1 AU is taken into account). We found that we could eliminate these background neutrons by tightening the geometrical constraints on the data. Background neutrons can come directly from the earth's atmosphere, from the spacecraft or from the instrument itself via neutron initiated cascades in the upper D1 detector. Specifically, we require that a neutron event must have a measured ϕ less than 15° and also that the scattered neutron velocity vector be no closer to the earth's limb than 35°. These two restrictions reduce the effective field-of-view of the telescope and severely restrict the neutron events which could be attributable to the earth albedo. These selection criteria greatly reduce the number of analyzable neutron events. For the June 9 flare after making this data cut there were no longer any neutrons which originated before impulsive phase. A few events, though, had production times after the impulsive phase. These we take as background neutrons rather than as solar. Twenty one neutron events were contained in the impulsive phase time interval.

A complication occurs because the tighter selection criteria are not the same as those used to analyze the neutron calibration data on which we base the efficiencies. The calibration data were only constrained by the hardware; no additional geometrical constraints were imposed on the data. These additional constraints affect the net efficiency of the telescope. Consequently, the telescope efficiencies (Ryan *et al.* 1991) had to be adjusted to account for the reduced ϕ range.

The distribution of ϕ as measured by COMPTEL is limited at the low end by the energy threshold in the D1 detector, and limited at the high end by E_S, the energy of the scattered particle. In this case, the low-energy E_S threshold is determined simultaneously by the limit of the time-of-flight range and the neutron reaction threshold in NaI, both being approximately 10 MeV. The constraint of a maximum ϕ of 15° translates into a reduction in the solid angle of the scattering process in D1. We have corrected the efficiencies, therefore, with a simple solid angle factor. The correction is greatest for low neutron energies because the lower instrumental ϕ threshold is higher due to the scattering kinematics. The solid angle corrections corresponding to reducing ϕ from 35° to 15°, are 0.042, 0.11 and 0.15 for the calibration energies of 18.5, 35.7 and 77 MeV, respectively. The uncertainties in these numbers are considerable and could be as high as a factor of two. Better figures for these corrections, in addition to the total efficiencies, await Monte Carlo telescope simulations.

After correcting the efficiencies, the differential flux was calculated and then corrected for the loss of neutrons through β^- decay over the 1 AU flight path. The resulting differential flux was then integrated over energy yielding a time-integrated neutron flux of 2×10^{28} n-sr^{-1} over the energy range of 15 to 80 MeV. By far, the largest uncertainty in the integrated flux arises from the extrapolation of prototype COMPTEL efficiencies to those of the flight telescope and the subsequent analytical corrections to those efficiencies. Therefore, the flux value stated above is only good to about a factor of three. Some small number of background neutron events are present at times later than the impulsive phase, but this effect is small compared to the uncertainties in the net detection efficiencies. The integrated flux figure of 2×10^{28} n-sr^{-1} is more than an order of magnitude below the spectrum published by Evenson, Meyer, and Pyle (1983) for the 1982 June 3 solar flare. That spectrum from 20 to 100 MeV was constructed

from the measurement of neutron-decay protons in interplanetary space. Based upon the difference between our value and the spectrum of Evenson *et al.*, we can conclude that there should be no measurable signal in any ground level neutron monitor as there was for the 1982 June 3 flare, which was measurable at the few σ level.

6. Conclusions

(1) The sun was imaged in γ-rays for the first time.

(2) The first direct energy measurement of solar neutrons was performed.

(3) The γ-ray fluence in the nuclear line range of 4-8 MeV was approximately 30 γ-cm^{-2}. Within errors this equals the fluence in the 2.2 MeV line, making it consistent with many flares measured by SMM (Forrest, priv. comm.).

(4) The integrated neutron spectrum from 15 to 80 MeV is on the order of 2×10^{28} n-sr^{-1} at the sun.

(5) The neutron emission was consistent in time with the γ-ray emission, i.e. from 0136 - 0150 UT. There is strong evidence against precursor neutron emission. Prolonged emission after the impulsive phase appears to be consistent with background.

(6) The neutron background measured by COMPTEL was surprising large and required severe data cuts to eliminate, reducing the effective area accordingly. Consequently, we have revised our estimate of the neutron sensitivity to ~ 6 n-cm^{-2} for a 20 minute observation, or equivalently, 5×10^{-3} n-cm^{-2}-s^{-1} in the range of 15 to 80 MeV.

7. References

den Herder, J.W., H. Aarts, K. Bennett, H. de Boer, M. Busetta, W. Collmar, A. Connors, R. Diehl, W. Hermsen, J. Ryan, M. Kippen, L. Kuiper, G. Lichti, J. Lockwood, J. Macri, M. McConnell, D. Morris, R. Much, V. Schoenfelder, G. Stacy, H. Steinle, A. Strong, B. Swanenburg, B.G. Taylor, M. Varendorff, C. de Vries, and C. Winkler 1991, these proceedings.

Evenson, P., P. Meyer, and K.R. Pyle 1983, *Ap. J.*, **274** : 875.

Muraki, Y., K. Murakami, M. Miyazaki, K. Mitsui, S. Shibata, S. Sakakibara, T. Sakai, T. Takahashi, T. Yamada, and K. Yamaguchi 1991, submitted to *Ap. J. (Letters)*,

Murphy, R.J., and R. Ramaty 1984, *Adv. Space Res.*, **4** : 127.

Ryan, J.M., H. Aarts, K. Bennett, R. Byrd, C. de Vries, J.W. den Herder, A. Deerenberg, R. Diehl, G. Eymann, D.J. Forrest, C. Foster, W. Hermsen, J. Lockwood, G. Lichti, J. Macri, M. McConnell, D. Morris, V. Schönfelder, G. Simpson, M. Snelling, H. Steinle, A. Strong, B.N. Swanenburg, T. Taddeucci, W.R. Webber, and C. Winkler 1991, *Proc. Workshop on Gamma Ray Astron.*, Erice, Italy.

Ryan, J.M., V. Schönfelder, R. Diehl, G.G. Lichti, H. Steinle, B. Swanenburg, H. Aarts, A. Deerenberg, W. Hermsen, G. Kiers, J. Lockwood, J. Macri, D. Morris, G. Simpson, K. Bennett, G. Eymann, M. Snelling, C. Winkler, R. Byrd, C. Foster, and T. Taddeucci 1987, *Proc. 20th Intl. Cosmic Ray Conf. (Moscow)*, **4** : 425.